Reference: *Biol. Bull.* **199:** 29–40. (August 2000)

Frog Lim-1-like Protein Is Expressed Predominantly in the Nervous Tissue, Gonads, and Early Embryos of the Bivalve Mollusc *Mytilus galloprovincialis*

MARIO TORRADO AND ALEXANDER T. MIKHAILOV*

Developmental Biology Unit, Institute of Health Sciences, University of La Coruña, As Xubias, La Coruña 15006, Spain

Abstract. In a few well-known cases, the biological consequences of the disruption of *lim-1* homeodomain (HD) genes have demonstrated the important roles of these genes in vertebrate development, especially in the nervous tissue, kidney, and gonads. Functional assay approaches require information not only about *lim-1* gene organization, but also about properties and tissue localization of Lim-1 proteins. Although *lim-1* genes have been identified in certain phyla of invertebrates, no information is available on Lim-1 proteins and genes in bivalve molluscs. Our study represents the beginning stage of identification of the Lim-1-related proteins in marine bivalves. Using antibodies against the C-terminal region of the *Xenopus laevis* Lim-1 protein, we describe cross-reactive antigen patterns in adults and early embryos of the mussel *Mytilus galloprovincialis*, as well as in sea urchin and chick embryos. In adult mussels, nervous ganglia and gonads display the most prominent Lim-1 immunoreactivity. Further, the antibodies verified the prediction that mussel Lim-1 antigens, like Lim-1 HD proteins in general, can be localized in the nucleus. Moreover, antibody detection allowed us to identify the Lim-1-like antigens in unfertilized mature eggs, as well as in very early embryos of bivalve molluscs and sea urchins (*Strongylocentrotus purpuratus*). In mussel eggs and embryos, Lim-1 antigens are expressed in multiple forms (40, 45, and 65 kDa), as detected by SDS-PAGE followed by Western blot. Taken together, the observations emphasize the conservation of the Lim-1 protein expression pattern in the nervous tissue and gonads of different animal groups, and demonstrate that Lim-1-like polypeptides can be maternally accumulated in eggs and, therefore, are present in very early embryos before zygotic expression of the genes begins.

Received 13 December 1999; accepted 8 May 2000.

* To whom correspondence should be addressed: E-mail: margot @udc.es

Abbreviations: LIM, an abbreviation derived from the names of three homeodomain transcription factors, containing a cysteine-rich zinc-finger domain (*i.e.*, LIM-domain): **L**in-11 of *Caenorhabditis elegans*, **I**sl-1 of the rat, and **M**ec-3 of *C. elegans*; MW, molecular weight; SDS-PAGE, sodium dodecylsulfate polyacrylamide gel electrophoresis; HD, homeodomain.

Introduction

A cysteine-rich zinc finger domain, named LIM, was first identified in the *Caenorhabditis elegans* homeobox genes *lin-11* and *mec-3*, and in the rat DNA binding factor *Isl-1*. Then the LIM domain was found in a variety of proteins including transcription factors, cytoskeletal proteins, and LIM kinases (Dawid *et al.*, 1998; Bach, 2000). LIM domains appear to play a primary role in protein-protein interactions, through the formation of dimers with identical or different LIM domains or by binding distinct proteins (Breen *et al.*, 1997; Dawid *et al.*, 1998; Curtis and Heiling, 1998; Hobert and Ruvkun, 1998; Hobert and Westphal, 2000).

Phenotypic analysis of patterns of *lim* gene expression reveals that the genes can participate in a number of important events in early embryonic development, as well as in cell fate determination and cell differentiation at advanced stages of organogenesis. Moreover, some *lim* genes are constitutively expressed in adult tissues, where they may contribute to certain tissue-specific functions (Dawid *et al.*, 1998; Hobert and Westphal, 2000). The early and late ontogenetic expression phases of *lim* genes suggest that they have multiple and distinct functions at different stages of the animal life cycle. In the latter context, the LIM containing homeodomain (HD) *lim-1* genes have been most extensively studied in a range of animals.

Lim-1 encodes a protein with a pair of LIM domains located N-terminal to the HD. In vertebrates, *lim 1* was originally identified in the frog, *Xenopus laevis*, as *Xlim 1* (Taira *et al.*, 1992). In *X. laevis*, the *Xlim-1* is expressed in

the Spemann's organizer during gastrula stages, and in late embryos primarily in the nervous system and kidney (Taira *et al.*, 1992, 1994, 1997; Wallingford *et al.*, 1998; Carroll *et al.*, 1999a; Carroll and Vize, 1999). Similar patterns of *lim-1* expression have been observed in fishes (Toyama *et al.*, 1995; Carroll *et al.*, 1999b), chickens (Tsuchida *et al.*, 1994), mice (Fujii *et al.*, 1994; Shawlot and Behringer, 1995; Li *et al.*, 1999), rats (Furuyama *et al.*, 1994; Karavanov *et al.*, 1998), and humans (Dong *et al.*, 1997). The biological consequence of the disruption of *lim-1* HD genes or modifications of their expression patterns have demonstrated the crucial role of these genes in development, especially in the nervous tissue, kidney, and gonads (Shawlot and Behringer, 1995; Shawlot *et al.*, 1999; Taira *et al.*, 1997; Carroll and Vize, 1999).

In invertebrates, *lim-1* related genes have been identified in nematodes, fruit flies, and sea urchins. The *lin-11* gene of *C. elegans* (the closest homolog of amphibian and mammalian *lim-1*) is expressed in different subsets of neurons and in the vulva, and it is essential for uterine morphogenesis (Hobert *et al.*, 1998; Hobert and Westphal, 2000; Newman *et al.*, 1999). In *Drosophila*, the gene termed *dlim 1* is expressed in the head, the brain lobes, and in neurons of the ventral nerve cord (Lilly *et al.*, 1999). The *lim-1*-related HD gene of the sea urchin (*Hemicentrotus pulcherrimus*), *HpLim1*, is detected in early embryos and involved in the differentiation of endoderm, mesenchyme, and aboral ectoderm (Kawasaki *et al.*, 1999).

Thus, although expression in neural tissues seems to be a common feature of Lim-1-related HD factors in both vertebrates and invertebrates, most of these factors are also characterized by their expression in excretory and reproductive organ systems. These expression phenotypes have been described mainly at the molecular level by analysis of *lim-1* gene transcription patterns. An alternative approach is the analysis of post-translational Lim-1 expression by immunochemical methods. This approach makes it possible to measure this factor at the protein level in different cell types and to detect other tissues that express the polypeptide at different stages of development and in the adult state (Karavanov *et al.*, 1996; Brown *et al.*, 1999; Lilly *et al.*, 1999; Shimono and Behringer, 1999; Mauch *et al.*, 2000).

To our knowledge, no information is available on Lim-1 proteins (genes) in marine bivalve molluscs, although such data would be useful for further comparative analysis of Lim-1 expression patterns and functions in invertebrates and vertebrates (Hobert and Westphal, 2000). Our study represents the beginning stage of the identification of Lim-1-related proteins in bivalve molluscs. We describe the distribution patterns of immunoreactive Lim-1-like proteins in adults and early embryos of the mussel *Mytilus galloprovincialis*. We also report the first examination of Lim-1 antigen signals in sea urchin (*Strongylocentrotus purpuratus*) embryos, as well as in different compartments of the chick embryo brain.

Materials and Methods

Animals and embryos

Adult mussels (*Mytilus galloprovincialis*) and sea urchins (*Strongylocentrotus purpuratus*) were purchased during the spawning season (April–May of 1999) from commercial suppliers in La Coruña (Galicia, NW Spain). Published procedures (Sprung and Bayne, 1984; Holland and Holland, 1993; Mikhailov *et al.*, 1996) were followed for stripping of animals to obtain oocytes and sperm and for the subsequent *in vitro* fertilization and culture of embryos. At each chronological stage, the bulk of the embryos were re-collected, placed on ice, and typed morphologically under a dissecting microscope (Nikon). The embryos, selected according to morphology, were put into centrifuge tubes containing sterile seawater and permitted to settle to the bottom of tubes or pelleted by low-speed centrifugation; then the upper solution was discarded. Fertilized chicken (*Gallus gallus*) eggs were obtained from the cooperative chick network hatchery (Ferrol, Province of La Coruña, Galicia) and incubated at 37°C. Different brain regions (forebrain, optic lobes, and cerebellum) were microsurgically isolated in cold minimum essential medium (MEM; Gibco) and pelleted by low-speed centrifugation.

Tissue dissection and processing

Before use, adult mussels (*M. galloprovincialis*) were kept in a dry state for 1 h at 4°C. Mussels were opened with the aid of scalpel and placed on ice; a small portion of gonad material was microscopically examined to determine the sex of the individual. Different tissues and organs (gonad, foot, labial palps, hepatopancreas, gill, and fragments of posterior adductor muscle) were excised, rinsed in sterile seawater, and blotted on sterile filter paper. To obtain cell suspensions of sperm or oocyte, gonad follicle biopsy was performed as described in Torrado and Mikhailov (1998). Then, follicle luminal masses were aspirated and resuspended in ice-cold sterile seawater; the released cell suspension was microscopically tested for the presence of spermatozoa or oocytes. The sperm suspension was then centrifuged ($100 \times g$, 5 min, 2°C), the oocytes were permitted to settle to the bottom of the tubes, and the rinse solution was discarded. For some experiments, gonad collecting tubules (with adjacent connective tissue) were dissected manually from the ripe male or female gonad and the excised tissue was microscopically examined to definitively determine the absence of gametes (spermatozoa or oocytes) in the tubule lumen. Isolated tissues were additionally shaken in ice-cold sterile seawater for 20 min; after settling, rinse solutions were discarded. Pedal ganglia (see Fig. 4A) were microsurgically dissected under a stereomicroscope (Nikon), pooled in ice-cold sterile seawater, and pelleted by low-speed centrifugation. When the samples were not homogenized immediately, they were stored at −85°C for several days.

Spent male gonads were sampled in 1998, and the corresponding frozen and Bouin-fixed tissue fragments were stored in liquid nitrogen and ethanol (70%), respectively.

Sample preparation

Mussel and sea urchin eggs and embryos were resuspended in cooled deionized water containing 2 m*M* EDTA (Merck), 6 *M* urea (Merck), and the protease inhibitor cocktail P2714 (Sigma). The supernatants obtained after centrifugation (30,000 × *g*, 8°C, 30 min) were mixed with SDS sample buffer containing the protease inhibitor cocktail, kept for 1 h at room temperature, and stored at −30°C until use. All other tissue samples were first homogenized in 1:5 (v/v) ratio in 100 m*M* Tris (Sigma), 2 m*M* EDTA (Merck) solution, containing the protease inhibitor cocktail. After centrifugation (10,000 × *g*, 2°C, 30 min), the supernatants were discarded, and the pellets were then re-extracted and assayed as described for embryos.

Antibodies

Anti-XLim-1 antibodies were a generous gift from Dr. A. A. Karavanov and Prof., Dr. I. Dawid. These polyclonal rabbit antibodies produced against the C-terminal region of the XLim-1 downstream of the HD (amino acids 265-403) (Taira *et al.*, 1992) have been characterized and shown to cross-react with Lim-1 proteins of fishes, mice, rats, and humans (Karavanov *et al.*, 1996, 1998). Gamma-globulin fraction was obtained from anti-XLim-1 serum with the aid of the Mab Trap G II Kit for antibody purification (Pharmacia), according to the manufacturer's protocol. The fraction was concentrated using concentrator units (Millipore), supplemented by glycerol (Merck) at a final concentration of 50%, and stored at −20°C in aliquots. Chemicon has recently commercialized these anti-XLim-1 antibodies.

Protein determination

Protein concentration was measured (Ultrospec 1000E spectrophotometer, Pharmacia) according to the Bradford method using rabbit immunoglobulin G (Sigma) or bovine serum albumin (Sigma) as standards.

SDS-PAGE assays

For all separations, the Mini-Protean II electrophoretic cell (Bio-Rad) was used. Samples were electrophoresed using 5% stacking and 10% resolving Tris-glycine SDS-polyacrylamide gels (Bio-Rad). The gels were stained with Coomassie blue R250 (Sigma) or electrophoretically transferred to membranes. The apparent molecular weights of the bands were determined by comparing low and high molecular weight calibration kits (Pharmacia) in the same gel. A micro-preparative variant of SDS-PAGE was performed as previously described (Mikhailov *et al.*, 1997) using a Mini-Protean II comb with one reference well. After electrophoresis, the reference gel strip was stained and used for isolating the Lim-1-containing fraction in the remaining gel slab. Alternatively, whole gel slabs were stained with Coomassie solution (0.0004% in 20% methanol and 3% acetic acid), and fractions of interest were cut out (Mikhailov *et al.*, 1996). The protein was eluted from gel fractions so obtained using a model 442 electro-eluter (Bio-Rad) in accordance with the manufacturer's recommendation; eluted solutions were concentrated using microconcentration units (Amicon, the 30-kDa cut-off membrane).

Blotting assays

Proteins resolved in 10% SDS-PAGE were transferred to nylon (Nytran, Schleicher and Schuell) or nitrocellulose (Optitran, Schleicher and Schuell) membranes by routine methods (Mikhailov *et al.*, 1997) using the mini Trans-Blot cell (Bio-Rad). Protein loading and localization of molecular weight standards was verified by membrane staining with amido black (Merck) or Ponceau S (Sigma). For immunodetection, the blots were incubated in blocking solution containing 20% of normal horse serum (Sigma) at room temperature for 1 h and further assayed as described in Mikhailov and Simirsky (1991). As primary antibodies, rabbit anti-XLim-1 or rabbit pre-immune (negative control) gamma-globulin fractions were used at appropriate dilutions. Peroxidase-labeled anti-rabbit immunoglobulins (Sigma) were used as the second-stage reagent, and diaminobenzidine (Sigma) was used to develop the blots. The relative amounts of antibody-labeled proteins were quantified by densitometry (GS-700 densitometer, Bio-Rad) and image software (Molecular Analysis, Bio-Rad). For total carbohydrate detection, blots were treated with an Immun-Blot kit (Bio-Rad) for glycoprotein detection as described (protocol 1A) by the manufacturer; chicken egg ovalbumin (Sigma) and rabbit liver carboxylesterase (Sigma) were used as positive controls. For a precise comparison of the position of the glycoprotein signal with that of Lim-1 immunoreactivity, the blot membrane was cut (along the direction of electrophoretic separation) at the middle of the run pocket width; one half was treated with Immun-Blot kit and the other with anti-XLim-1 antibodies (see Fig. 3C,D).

Deglycosylation assay

Extracts and Lim-1-containing fractions of mussel pedal ganglia and forebrains of 16-day-old chick embryos were desalted (using Microcon units), re-dissolved in 250 m*M* sodium phosphate (Merck), pH 6.0, and treated with an enzymatic deglycosylation kit (Bio-Rad) according to the manufacturer's denaturing protocol. Briefly, both neuraminidase (EC 3.2.1.18) and *O*-glycosidase (EC 3.2.1.97) were first added to the reaction vials; after the incubation and denaturation step, *N*-glycosidase F (EC 3.5.1.52) was added to the mixture. To determine deglycosylation efficiently, samples (before and after deglycosylation) were

subjected to SDS-PAGE followed by Coomassie staining (to detect the shift in band mobility) or blotting. Blots were treated with an Immun-Blot kit (Bio-Rad) for glycoprotein detection to additionally check the efficiency of the deglycosylation reaction. Bovine fetuin (Bio-Rad) and rabbit liver carboxylesterase (Sigma) were used as positive controls.

Ultrafiltration procedures

Lim-1-containing fractions isolated from mussel pedal ganglia and forebrains of 16-day-old chick embryos were subjected to subsequent ultrafiltration using Microcon micro-units with 100-kDa and 50-kDa cut-off YM membranes (Amicon) according to the manufacturer's recommendation. Bovine serum albumin (Sigma) and chicken ovalbumin (Sigma) solutions (1 mg/ml) were used as reference proteins. To prevent aggregation, urea (Merck) and SDS (Bio-Rad) were added to starting protein solutions at final concentrations of 6 *M* and 1%, respectively. Each sample was first applied on the Microcon-100 unit and centrifuged at 2500 × *g* for 30 min at 10°C. The resulting filtrate was then introduced into a sample reservoir of the Microcon-50 unit and centrifuged at 12,000 × *g* for 20 min at 10°C. The volume of each retained and filtered fraction so obtained was adjusted to that of the starting sample, and the solutions were subjected to SDS-PAGE followed by Western blot with anti-XLim-1 antibodies.

Immunocytochemistry

Mussel pedal ganglia were fixed in 100 m*M* 3-(*N*-morpholino) propane sulfonic acid (MOPS; Sigma), 2 m*M* $MgSO_4$ (Panreac), 2 m*M* EGTA (Merck), 3.8% formaldehyde (Panreac) for 1 h at room temperature. Standard histological techniques were used for sample dehydration, embedding in paraffin, sectioning at 6 μm, deparaffinization, and rehydration (Mikhailov and Simirsky, 1991). The slides were precoated with 3-aminopropyltriethoxysilane (Sigma). Prior to immunostaining, sections were blocked with 20% normal horse serum in 50 m*M* Tris-HCl, pH 8.0. Sections were then incubated with different dilutions of the anti-XLim-1 immunoglobulin fraction (3 h at room temperature or overnight at 4°C) and secondary antibodies conjugated to alkaline phosphatase (Boehringer-Mannheim). Antibody dilutions were prepared in blocking solution. All incubations were followed by six washes (10 min in each) in 50 m*M* Tris-HCl, pH 8.0. Staining was developed using 5-bromo-4-chloro-2-indolyl-phosphate (Sigma) and 4-nitro blue tetrazolium chloride as substrates (Sigma) as described in Karavanov *et al.* (1996). The sections were mounted in Permount (Fisher) and examined under the Nikon Microphot microscope. Control experiments were included (1) omitting anti-XLim-1 antibodies, (2) replacing the latter by normal rabbit immunoglobulins (Sigma), and (3) using anti-XLim-1 antibodies preadsorbed by fixed pedal ganglia or by foot tissue of *M. galloprovincialis*. Fixation was done in 3.8% formaldehyde as above, followed by a methanol wash. Using micro-forceps, fixed tissues were ground, rehydrated in 50 m*M* Tris-HCl, pH 8.0, blocked in blocking solution for 2 h, pelleted by a low-speed centrifugation, resuspended in anti-XLim-1 antibody solution (at 1/50 or 1/200 dilution), and incubated overnight at 4°C. For some experiments, anti-XLim-1 antibodies were depleted prior to staining by incubation at 1/50 dilution with hyperfixed *Xenopus laevis* embryos (this was performed by Dr. A. A. Karavanov and Dr. A. T. Mikhailov in the laboratory of Prof. I. Dawid).

Histological analysis

A portion of male ripe and spent gonads of *M. galloprovincialis* was fixed in Bouin's solution, embedded in paraffin, cut into 6-μm sections, and stained with hematoxylin-eosin; the gonadosomatic index was estimated from the sections and expressed as the percentage of the gonad occupied by follicle structures (Mikhailov *et al.*, 1996; Torrado and Mikhailov, 1998).

Results and Discussion

In this study we used rabbit polyclonal antibodies against a C-terminal region (as an immunogen) of the *Xenopus laevis* Lim-1 protein (*i.e.*, anti-XLim-1 antibodies). It has been shown that these antibodies detect the Lim-1 protein in *X. laevis* and also cross-react with Lim-1 polypeptides of the mouse (Karavanov *et al.*, 1996; Shimono and Behringer, 1999) and rat (Karavanov *et al.*, 1998). These studies have also demonstrated the high specificity of the antibodies to Lim-1 proteins and the absence of any discrepancy between the expression patterns of protein and mRNA. Note that the transcriptional activation domain of *Xlim-1* resides in its carboxyl terminus (Breen *et al.*, 1997).

Although it is generally accepted that the C-terminal peptide is a good choice for the production of antibodies specific to a protein of interest (Hancock and Evan, 1992), we decided to test, additionally, the degree of "specificity" of the *Xlim-1* C-terminal region (used as an immunogen) for Lim-1 proteins. Using the BLAST program (Altschul *et al.*, 1997), we performed alignments of the C-terminal sequence of *Xlim-1* with all the protein sequences listed in the SWISSPROT database (Bairoch and Apweiler, 2000). The most similar (similarity 80%–90%; Fig. 1) sequences, which were aligned first, are those of the fish, chick, mouse, and human Lim-1. Frog and fish Lim 5 factors are characterized by significantly lower primary structural similarity (47% and 46%, respectively) to the *Xlim-1* C-terminus sequence. It is significant that the regions of homology reside only in the C-terminus of the sequences mentioned above. Other sequences returned by the BLAST program displayed values of similarity with the C-terminus of *Xlim-1* (used as a query) that are not distinguishable from those

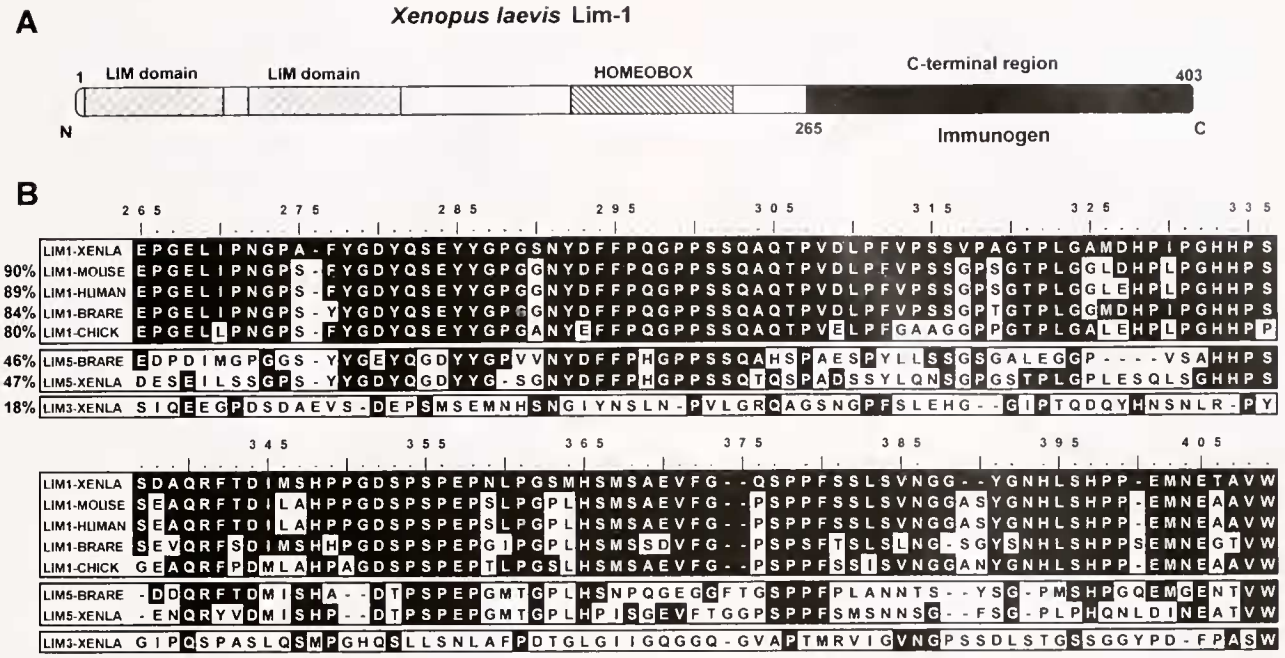

Figure 1. Multiple alignment of the deduced amino C-terminal sequence of *Xlim-1* with those identified from BLAST search comparisons. (A) Schematic structure of the frog Lim-1 deduced from the previously published *Xlim-1* sequence (Taira *et al.*, 1992). The C-terminal region, which was used to generate anti-XLim-1 antibodies (Karavanov *et al.*, 1996), is shown in black. (B) The complete sequence of the *Xenopus* (XENLA) C-terminus is shown aligned with those of mouse, human, zebrafish (BRARE), and chick Lim-1s as well as with *Xenopus* Lim-5 and Lim-3 and zebrafish Lim-5. All the protein sequences were obtained from the SWISSPROT database (Bairoch and Apweiler, 2000). Black—identical amino acid residues. Dash—gaps. Comparison shows that both the size and the sequence of the XLim-1 C-terminus are highly similar (80%–90% of similarity; extent internal homology above seven amino acid residues) to that of Lim-1 proteins from other species. At the same time, the XLim-1 C-terminal sequence reveals no more than 50% of similarity (extent internal homology below seven amino acid residues) with that of Lim-5 proteins. No significant similarity was observed in the case of the *Xenopus* Lim-3.

expected by chance (Fig. 1, see *Xenopus* Lim-3 as an example).

It is generally accepted that short peptides (below about seven amino acid residues) are of insufficient size to function as immunogenic and antigenic epitopes (Hancock and Evan, 1992). Using the CLUSTAL W program (Thompson *et al.*, 1994), we performed a multiple sequence alignment of the XLim-1 C-terminal region with that of the Lim-1 and Lim-5 proteins identified from BLAST searches (see above). As shown (Fig. 1), the XLim-1 C-terminus shares a high sequence homology with a number of Lim-1 proteins but not with Lim-5 factors. Given the above criteria, it is probable that the XLim-1 C-terminus (used as immunogen) could generate successful antibodies characterized by a high cross-reactivity with Lim-1 proteins in other species. At the same time, it may be predicted that antibodies against the XLim-1 C-terminus possess a much lower cross-reactivity with Lim-5 proteins. Note that anti-XLim-1 antibodies used in this study cross-react with Lim-1 factors from various species but do not cross-react with the closely similar XLim-5 protein on tissue sections (Karavanov *et al.*, 1996).

Collectively, the data indicated that the *Xlim* C-terminal sequence (used as an immunogen to generate anti-XLim-1 antibodies) is highly conserved among most of other known *lim-1* genes and seems to be diagnostic for their protein products. This would in turn account for the use of the corresponding antibodies in selective (discriminative) immunochemical screening of Lim-1-related proteins in different species. This suggestion is supported by the results of application of anti-XLim-1 antibodies for immunocytochemical Lim-1 protein detection in frog, mouse, and rat tissues (Karavanov *et al.*, 1996, 1998; Shimono and Behringer, 1999).

Anti-Xlim-1 antibodies cross-react with mussel, sea urchin, and chick tissue antigens

SDS-PAGE followed by immunoblot analysis of a protein extracted from isolated pedal ganglia of *Mytilus galloprovincialis*, mature oocytes of *Strongylocentrotus purpuratus*, and brain tissues of chick embryos revealed a single band with an apparent molecular weight (MW) of approximately 65, 70, and 65 kDa, respectively (Fig. 2). Note that the open reading frame of the chicken (Tsuchida *et al.*,

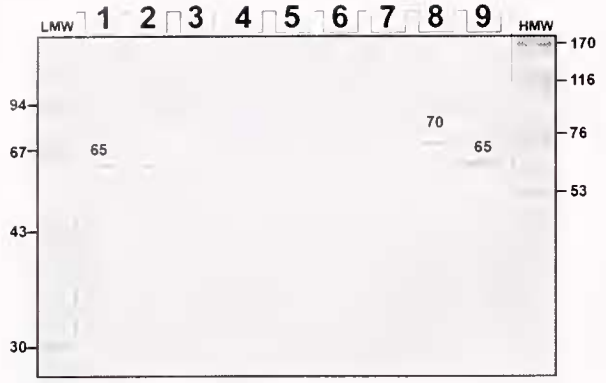

Figure 2. Cross-reactivity of anti-XLim-1 antibodies with mussel, sea urchin, and chick tissue antigens. Equal amounts (about 100 μg/pocket) of total protein extracted from different tissues were resolved in a 10% SDS-PAGE, blotted on membranes, and probed with anti-XLim-1 antibodies at 1/500 dilution. Membrane strips containing electrophoretically separated molecular weight markers were stained with Ponceau S. *Mytilus galloprovincialis* organs and tissues: Lane 1—male pedal ganglia; Lane 2—female pedal ganglia; Lane 3—male muscle adductor posterior; Lane 4—male gills; Lane 5—male foot; Lane 6—male hepatopancreas; Lane 7—male labial palps. Lane 8—*Strongylocentrotus purpuratus* eggs. Lane 9—forebrain tissues of 16-day-old chick embryos. LMW and HMW—low and high molecular weight calibration kit proteins (30–170 kDa), respectively. 65 and 70—molecular weights of antibody-labeled proteins, kDa.

1994) and sea urchin (Kawasaki *et al.*, 1999) *lim-1* gene encodes a protein with a predicted MW about of 45 kDa. The high MW value of the Lim-1 antigens is apparently not due to aggregation with other molecules, because it did not change when the antigens were extracted and electrophoretically analyzed in the presence of 6 *M* urea. In addition, observed low migration of mussel and chick Lim-1 antigens in SDS-PAGE is not due to their interactions with non-polymerized products of polyacrylamide gel (data not shown).

The discrepancy between the theoretical (45 kDa) and apparent (65 kDa) MWs of the Lim-1 antigens could be due to post-translation modifications in the protein molecules. In *X. laevis*, three Lim-1 bands were detected (by SDS-PAGE followed by Western blot with anti-XLim-1 antibodies) in embryos injected with the full-length synthetic *Xlim-1* mRNA. The fastest band of the "triplet" co-migrated with the protein product obtained from the same mRNA in a cell-free translation system, whereas other fractions were characterized by a lower electrophoretic migration. The latter suggested that a portion of the protein could be subject to post-translational modifications in the embryo (Karavanov *et al.*, 1996).

Using the ScanProsite tool (Hofmann *et al.*, 1999), we found that the *Xlim-1* sequence contains three potential sites for glycosylation, one of which resides in the C-terminus of the protein. By analogy with the XLim-1 protein, we proposed that mussel and chicken Lim-1 antigens run more slowly than predicted in SDS-PAGE, probably due to a glycosylation of the corresponding proteins. To investigate this option, we performed two experiments. First, Lim-1-containing fractions isolated from mussel pedal ganglia and chick embryo brain tissues (Fig. 3A, B) were electrophoresed on SDS-PAGE, blotted onto nylon membrane, and treated with the Immun-Blot kit for glycoprotein detection. Although a portion of each fraction displayed positive staining, the zones corresponding to Lim-1 antigens were absolutely negative (see Fig. 3C, D). Next, the same fractions were treated with the Bio-Rad deglycosylation kit, which enzymatically cleaves all *N*-linked and most *O*-linked oligosaccharides from glycoproteins. Treated and untreated Lim-1-containing fractions were subjected to SDS-PAGE followed by Western blot. All comparisons failed to identify any change in electrophoretic mobility of treated Lim-1 antigens (Fig. 3E, F). Thus, the difference between the predicted (45 kDa) and the apparent (65 kDa) MW of the Lim-1 antigens studied is apparently not due to the post-translational glycosylation of protein products.

To begin characterizing effective size values, Lim-1-containing fractions of mussel pedal ganglia and chick embryo brains were subjected to a subsequent ultrafiltration using 100- and 50-kDa cut-off membranes (Fig. 3G). Since mussel proteins tend to aggregate during ultrafiltration (Mikhailov *et al.*, 1997), the SDS and urea were added to starting Lim-1 and reference protein (*i.e.*, bovine albumin and chicken ovalbumin) solutions. Using SDS-PAGE followed by Western blot, we found that about 50% of the Lim-1 immunoreactivity, characteristic of Lim-1-containing fractions, is retained by the 100-kDa cut-off membrane, whereas no more than 40% of the immunoreactivity is detected in the filtrate. The latter is completely retained by the 50-kDa cut-off membrane. Such retention and recovery patterns are more similar to those of bovine serum albumin (MW 67 kDa) than to those of chicken ovalbumin (MW 43 kDa). In particular, about 60% of the bovine albumin was retained by the 100-kDa cut-off membrane, whereas more than 70% of the chicken ovalbumin passed through the membrane (data not shown). This raises the possibility that the effective MW (size) of the Lim-1 antigens studied could be larger than the theoretical one (45 kDa).

Taken together, the results indicate that the apparent MWs of the Lim-1 polypeptides, immunochemically detected in *M. galloprovincialis* pedal ganglia, *S. purpuratus* embryos, and chick embryo brain tissues, seem to be 40% higher than those calculated from deduced amino acid sequences derived from sea urchin (Kawasaki *et al.*, 1999), chick (Tsuchida *et al.*, 1994), and frog (Taira *et al.*, 1992) cDNA *lim-1* clones. We could not find any reference to apparent MWs of the Lim-1 proteins detected in frog, sea urchin, and chick tissues. For the other family of the zinc-finger transcriptional factors, aberrantly high MW values (in SDS-PAGE) have been found to be due to the particular amino acid composition of the C- and N-terminal domains (Klenova *et al.*, 1997). Examination of amino acid composition of the chicken, sea urchin, and frog Lim-1 C-terminal

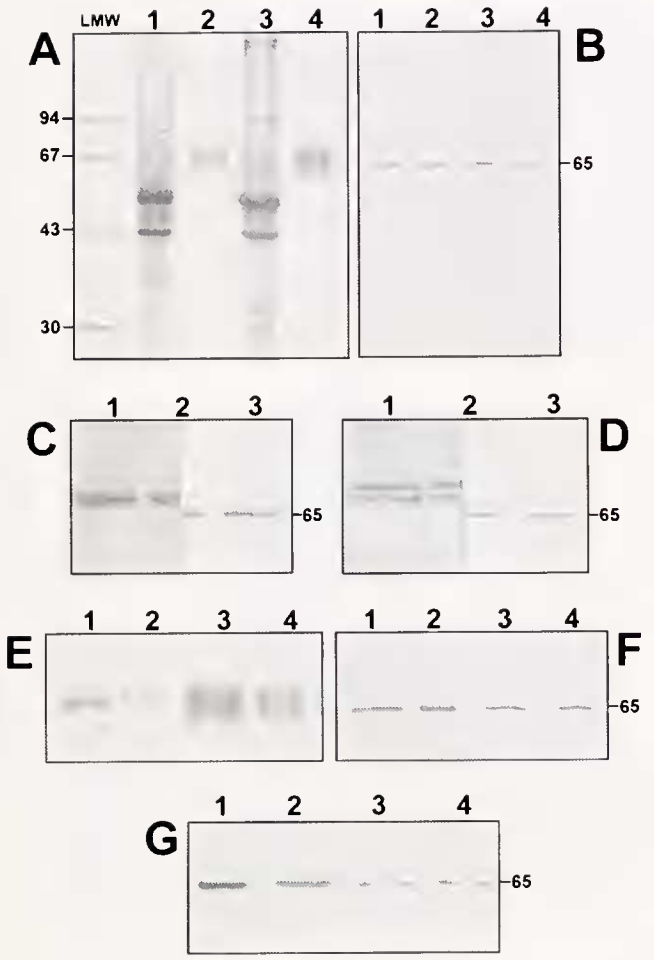

Figure 3. Characterization of mussel and chick Lim-1-like antigens. Lim-1-containing fractions isolated from mussel and chick tissues were subjected to SDS-PAGE followed by Western blot with anti-XLim-1 antibodies. Coomassie (A) and antibody (B) staining: Lane 1 and Lane 2—total extract and Lim-1-containing fraction of 16-day-old chick embryo forebrains, respectively; Lane 3 and Lane 4—total extract and Lim-1-containing fraction of *Mytilus galloprovincialis* pedal ganglia, respectively; LMW—low molecular calibration kit proteins (30–94 kDa). Note that fractions display the Lim-1 immunoreactivity similar to that of tissue extracts. In further experiments, chick (C) and mussel (D) Lim-1-containing fractions (Lanes 1, 2, and 3, respectively) were resolved in 10% SDS-PAGE and blotted on membranes. Each membrane was cut into two parts (see "Materials and Methods"): one part was treated with an Immun-Blot kit for glycoprotein detection (Lane 1 and a half of the Lane 2); the other (a half of the Lane 2 and Lane 3) was treated with anti-XLim-1 antibodies. Note that immunolabeled Lim-1 antigen bands do not reveal any glycoprotein-specific reaction. Next, chick and mussel fractions were treated with a deglycosylation kit and subjected to SDS-PAGE followed by Coomassie staining of the gel (E), or blotted on membranes followed by antibody staining of the membrane (F): Lane 1 and Lane 2—untreated and treated chick Lim-containing fraction, respectively; Lane 3 and Lane 4—untreated and treated mussel Lim-1-containing fraction, respectively. Note that the electrophoretic position of antibody-labeled bands in treated Lim-containing fractions corresponds to the 65-kDa value, as is the case for untreated fractions (see F; Lane 1 *versus* Lane 2, and Lane 3 *versus* Lane 4). Finally, chick Lim-containing fraction was subjected to subsequent ultrafiltration. Retained and filtered proteins were subjected to SDS-PAGE followed by Western blot with anti-XLim-1 antibodies (G). Immunostaining (signal quantitation, %): Lane 1—isolated Lim-1 fraction (100%), Lane 2—Lim-1 fraction retained by the 100-kDa cut-off membrane (~50%); Lane 3—Lim-1 fraction partially passed through the 100-kDa cut-off membrane (~40%); Lane 4—the latter retained by the 50-kDa cut-off membrane (~30%). 65—molecular weight of Lim-1-like antigens, kDa. Positions of bovine serum albumin (67 kDa) and chicken egg ovalbumin (43 kDa) are shown on (A).

regions revealed that they are enriched with proline (18%, 20%, and 17%, respectively). Since polypeptides with a high proline content can give abnormally high MW values by SDS-PAGE (Hames, 1990), we suggest that the proline-rich C-terminus of the Lim-1 proteins may be responsible, at least in part, for their behavior when analyzed by SDS-PAGE (as could be the case of Lim-1 antigens studied). It is unlikely that Lim-1-like tissue antigens detected in this work are multimeric forms or aggregates that include other components, because reducing agents were present at all stages of the separation. Further studies should elucidate the significance of our findings and explain the discrepancy between the apparent MW of Lim-1 proteins immunochemically detected in chicken and sea urchin tissues and that deduced from the coding region of the corresponding cloned cDNAs.

Mussel pedal ganglia and gonads display the most prominent Lim-1-like immunoreactivity

In adult *M. galloprovincialis*, the most prominent Lim-1 immunoreactivity examined by Western blot analysis was detected in the pedal ganglia and gonads, in both males and females (Figs. 2, 5, 6). A very weak immunostaining was observed in gills and muscle tissues but not in hepatopancreas, foot, or labial palps (Fig. 2). Pronounced Lim-1 antigen accumulation in mussel nervous tissues and gonads raises a question about its possible functional importance. In this respect, it is interesting to note that mice carrying a disruption of the *lim-1* gene (Shawlot and Behringer, 1995) fail to develop the head and also lack kidneys and gonads.

Immunohistochemical staining was used to further characterize the Lim-1 expression pattern in the mussel nervous tissue. Figure 4 illustrates the nuclear localization of the antigen in neurons of pedal ganglia. To avoid the possibility of nonspecific cross-reactivity, we used anti-XLim-1 antibodies depleted prior to immunostaining by incubation with hyperfixed *X. laevis* embryos. This procedure results in the decrease of background and the enhancement of the signal-to-noise ratio (Karavanov *et al.*, 1996). The positive immuno-signal of mussel nuclei was blocked by adsorption of anti-XLim-1 antibodies with fixed pedal ganglia but not with fixed *M. galloprovincialis* foot or hyperfixed *X. laevis* embryo, providing additional support for tissue-specificity of immunodetection of the antigen. We reason that observation of a Lim-1-like positive signal in nuclei of mussel pedal ganglia is consistent with the generally accepted

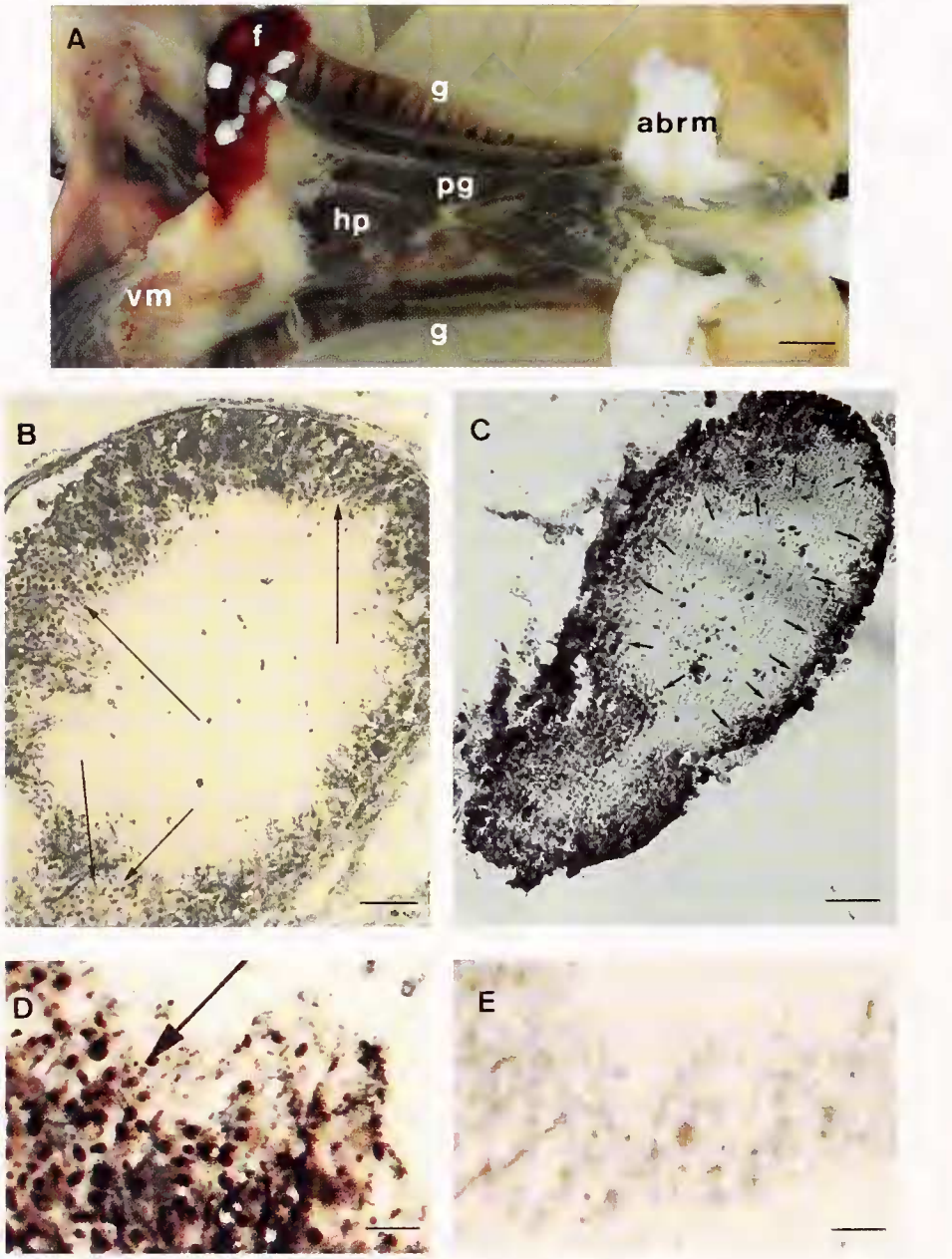

Figure 4. Tissue section visualization of Lim-1 immunoreactivity signal in *Mytilus galloprovincialis* pedal ganglia. (A) Localization of the pedal ganglion in the mussel. The anterior end of the animal is to the right; pg—pedal ganglion; g—gills; hp—hepatopancreas, f—foot; vm—visceral mass; abrm—anterior byssal retractor muscle. Ganglia were dissected, fixed, paraffin-embedded, and processed for immunohistochemistry using primary anti-XLim-1 antibodies and secondary antibodies conjugated to alkaline phosphatase. (B) Section treated with anti-XLim-1 antibodies depleted by hyperfixed *Xenopus laevis* embryos. Note the positive staining of nuclei (long arrows). (C) Section treated with anti-XLim-1 antibodies preadsorbed by fixed foot tissues of *M. galloprovincialis*. Short arrows point to a nuclear region (arranged on entire circumference of the ganglion) that is positive for anti-XLim-1 antibody staining. (D) Higher magnification of the section in (B), showing intensive immunostaining in isolated nuclei. (E) Section treated with anti-XLim-1 antibodies preadsorbed by fixed pedal ganglia of *M. galloprovincialis*: no immunoreactivity is observed in the nuclei (scale bar: A—5 mm; B—50 μm; C—100 μm; D and E—20 μm).

putative function of Lim-1 HD proteins as transcription factors.

In the *M. galloprovincialis* ripe male gonad, Lim-1 positive signals (*i.e.*, a major 60-kDa and a minor 65-kDa band) were detected in somatic gonad tissues, but not in sperm cells (Fig. 5A, C). In spent male gonads (*i.e.*, gonads that do

not contain sperm cells and consist of gonad tubules and mantle connective tissue) a very weak 60-kDa immunoreactivity was found. At the histological level, not only sperm but also mature Sertoli cells were undetectable in seminiferous tubules of the spent gonad (Fig. 5B). The results suggest that in mussel male gonad, the 60-kDa antigen is mainly associated with Sertoli cells. This finding is consistent with data on Lim-1 protein cell localization in the fetus testis of the rat (Karavanov *et al.*, 1996). The minor 65-kDa band seems to be also characteristic for gonad somatic tissue, although its precise cell association remains to be elucidated.

Next we questioned whether the Lim-1 distribution in the *M. galloprovincialis* female gonad was similar to that in the male gonad. In the female ripe gonad, antibody staining revealed two Lim-1-like antigens with MWs of approximately 65 and 40 kDa (Fig. 6). In the oocyte-free gonad portion, containing mainly collecting tubules and mantle mesenchyme cells, only the 65-kDa fraction was detected. In mature spawned oocytes, both the 65- and the 40-kDa Lim-1 antigens were found. The 40-kDa band does not appear to be an artifact of degradation caused by sample processing. Detection of the 40-kDa Lim-1 antigenic polypeptide in the mussel female gonad is perhaps not surprising, because the *X. laevis* ovary contains the 2.7-kb maternal *Xlim-1* mRNA that is smaller than the larger zygotic 3.4-kb transcript found in the adult brain (Taira *et al.*, 1992). It should be noted that in immature oocytes (obtained by biopsy of female gonad follicles), neither 65-kDa nor 40-kDa antigens were found (see Fig. 6, Lane 3).

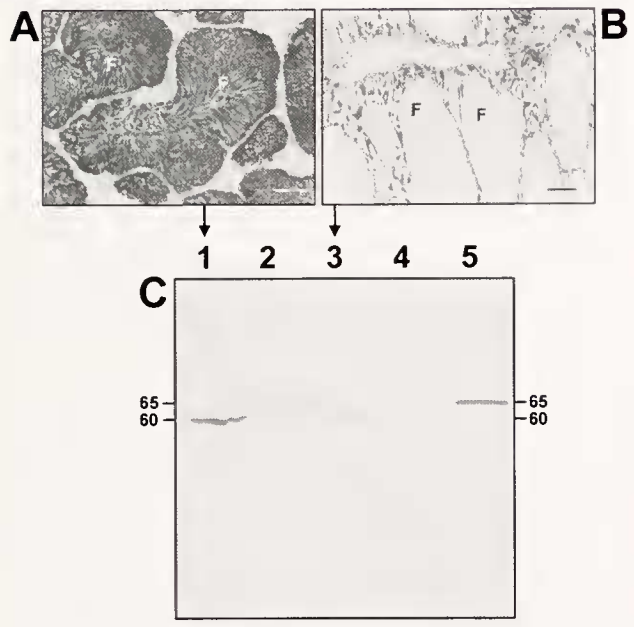

Figure 5. Analysis of Lim-1 antigen distribution in male gonads of *Mytilus galloprovincialis*. Histological sections of ripe male gonad before (A) and after (B) complete spawning (spent gonad). Note that the gonad samples are characterized by the same patterns of follicle (F) morphogenesis and gonadosomatic index values (in both samples, about of 90% of gonad volume was occupied by follicles) (scale bar—100 μm). (C) Extracts prepared from complementary gonad (Lane 1 and Lane 3; arrows) of the same animals, as well as from somatic tissues (Lane 2) and sperm cells (Lane 4) of the other ripe gonad before spawning, were subjected to SDS-PAGE followed by Western blot with anti-XLim-1 antibodies. Lane 1—gonad biopsy containing somatic tissue, gonad ducts, fluids, and sperm; Lane 2—gonad tube-free sample containing the mantle connective tissues only; Lane 3—spent gonad; Lane 4—mature sperm cells; Lane 5—optic lobe of 16-day-old chick embryos (reference). 60 and 65—apparent molecular weight values of Lim-1 antigens, kDa.

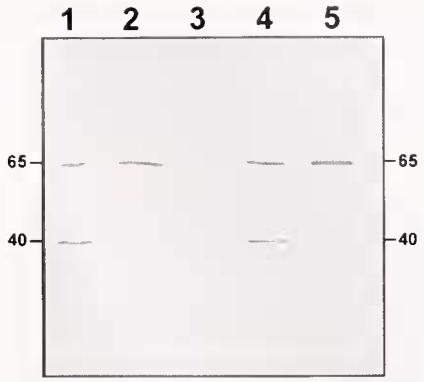

Figure 6. Analysis of Lim-1 antigen distribution in female gonads of *Mytilus galloprovincialis* using SDS-PAGE followed by Western blot with anti-XLim-1 antibodies. Lane 1—gonad biopsy containing somatic tissues, gonad ducts, fluids, and oocytes; Lane 2—gonad collecting ducts; Lane 3—immature oocytes obtained by biopsy of gonad follicles; Lane 4—spawned mature eggs; Lane 5—cerebellum of 16-day-old chick embryos (reference). 40 and 65—apparent molecular weight values of Lim-1 antigens, kDa.

It is clear from these results that the 65-kDa Lim-1 form in the female is associated with somatic tissues of the gonad just like the Lim-1 variants detected in the male gonad. At the same time, in the female gonad the 65-kDa antigen is also characteristic of mature eggs. The 40-kDa antigen, despite our uncertainty regarding its precise nature, is specific to the female germ line. It is likely that neither of the two antigens are expressed at early phases of oocyte differentiation, but are expressed and accumulated in eggs at terminal stages of their maturation. Therefore, the *M. galloprovincialis* female gonad pattern obtained by Western immunoblot analysis for Lim-1 antigens may be interpreted as a compound profile of the 65-kDa variant, which originates from both somatic tissues and eggs, and of the 40-kDa form, which seems to be specific to mature oocytes only.

Dynamics of Lim-1-like immunoreactivity during early development

Observations on female gonads have led us to examine the patterns and timing of maternal expression of the 65-kDa and 40-kDa Lim-1 variants during early development of *M. galloprovincialis*. Both antigen signals, already seen in unfertilized and fertilized eggs, persist in embryos during cleavage. At the beginning of the blastula stage, the inten-

sity of immunostaining of both the 65-kDa and the 40-kDa antigens decreases. In stereoblastulae, instead of these two Lim-1 antigenic variants, only 45-kDa immunoreactivity was observed. The latter was first detected in 8-cell embryos, and its intensity reached a maximum in blastulae (Fig. 7A).

Data from a variety of sources are consistent with the fact that zygotic transcription of *lim-1* genes begins before gastrulation at or very shortly after the midblastula transition (Taira *et al.*, 1992; Rebbert and Dawid, 1997; Curtiss and Heiling, 1998; Kawasaki *et al.*, 1999). It may be speculated that in mussels, the 65- and 40-kDa signals are due to Lim-1-related maternal molecules stored in the full-grown oocytes, whereas the 45-kDa protein reflects zygotic activity of the gene. Such an interpretation may explain why multiple Lim-1 antigen variants have been detected in embryos of *M. galloprovincialis* at early blastula stages, but there is no definitive proof. It remains to be established how the compound profile of Lim-1 protein variants relates to maternal and zygotic gene expressions as well as to possible post-translation modifications of the primary gene product (Karavanov *et al.*, 1996) or to the so-called premature termination of translation processes involving both untranslated and coding regions of the zinc-finger transcriptional factors (Klenova *et al.*, 1997).

In sea urchin embryos, expression of the *lim-1*-related gene (*Hplim-1*) has been studied at the transcriptional level (Kawasaki *et al.*, 1999), so we decided to examine the Lim-1 antigen dynamics in the course of sea urchin early embryogenesis. Levels of Lim-1 immunoreactivity during *S. purpuratus* development are shown in Figure 7B. A relatively high-abundance signal of the Lim-1 antigen, already seen in eggs, persists in embryos to the blastula stage, decreases dramatically in unhatched blastulae, and increases again in late (post-hatched) blastulae. In more advanced embryos (*i.e.*, at prism and pluteus stages), trace amounts of the Lim-1 antigen were detected. Although the developmental kinetics of the Lim-1 protein in *S. purpuratus* is quite similar to that of the *Hplim-1* mRNA in *H. pulcherrimus* (Kawasaki *et al.*, 1999), the most interesting finding revealed by Western blot is that the Lim-1 antigen is present at relatively high levels very early during development. Note that *H. pulcherrimus* fertilized eggs and cleavage embryos contain a trace amount of the *Hplim-1* mRNA that becomes abundant only at the blastula stage just after hatching (Kawasaki *et al.*, 1999).

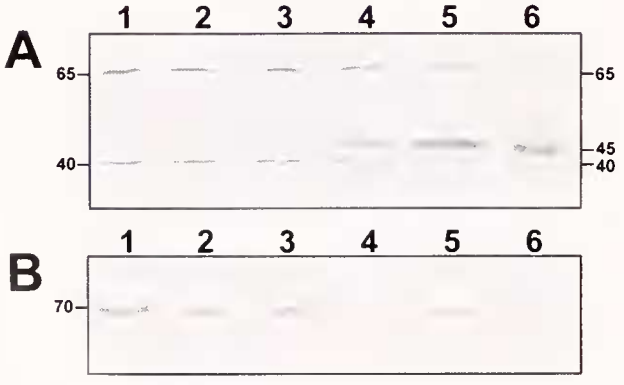

Figure 7. Patterns and timing of Lim-1 antigen expression in the course of early development of *Mytilus galloprovincialis* and *Strongylocentrotus purpuratus*. The extracts from eggs and embryos were subjected to SDS-PAGE followed by Western blot with anti-XLim-1 antibodies. (A) *M. galloprovincialis:* Lane 1—unfertilized eggs; Lane 2—fertilized eggs; Lane 3—4- and 8-cell embryos; Lane 4—16- and 32-cell embryos; Lane 5—early blastulae; Lane 6—stereoblastulae. (B) *S. purpuratus:* Lane 1—unfertilized eggs; Lane 2—fertilized eggs; Lane 3—8- and 16-cell embryos; Lane 4—unhatched blastulae; Lane 5—hatched blastulae; Lane 6—prism larvae. 40, 45, 65, and 70—apparent molecular weight values of Lim-1 antigens, kDa.

Thus, Lim-1-like polypeptides, which share common epitopes with the C-terminus of the frog XLim-1 protein, have been detected in both *M. galloprovincialis* and *S. purpuratus*. In these species, characterized by very different modes of early embryogenesis, the similar developmental kinetics of the Lim-1 antigens has been demonstrated. Whether this likeness leads to similar developmental consequences remains to be elucidated. In sea urchin embryos, ectopic expression of the *Hplim-1* inhibits endoderm and mesoderm differentiation, directing all embryonic cells to form oral ectoderm (Kawasaki *et al.*, 1999). It is widely accepted that maternally expressed gene products, stored in the egg, establish initial differences within the early embryo that, in turn, could contribute to further regionalization of the embryo body (Raff, 1996). The work described here particularly highlights the fact that in the marine invertebrates studied the Lim-1-like proteins maternally accumulated in the egg could persist after fertilization and be present in the early embryo long before zygotic expression of the genes is activated.

As mentioned above, the present study represents the first step in the identification and characterization of Lim-1-like proteins in marine bivalves. If it were accepted that the antibodies used recognize epitopes of the XLim-1 C-terminal sequence, then their cross-reactivity would appear to be specific for Lim-1-related proteins in many species (see Fig. 1). The corresponding immunochemical data obtained on rats (Karavanov *et al.*, 1996, 1998) and mice (Shimono and Behringer, 1999) confirm this assumption. Moreover, there is similarity between Lim-1 antigenic patterns observed in bivalves and those detected with the aid of the same antibodies in other species. This involves (1) the immunodetection of the Lim-1 protein in both ganglia and somatic gonads (bivalves—this work; rats—Karavanov *et al.*, 1996), and (2) the nuclear localization of Lim-1 immunoreactivity in tissue sections (bivalves—this work; frog and rats—Karavanov *et al.*, 1996; mice—Shimono and Behringer, 1999). In addition, the developmental dynamics of the Lim-1 antigen (this work) and *Hplim-1* mRNA (Kawasaki *et al.*, 1999) in sea urchin embryos appears to be very similar.

On the basis of the HD sequence similarity, vertebrate Lim-1 proteins, as well as Lim-5 and Lim-6 factors, have been included in the so-called LIN-11 class of LIM-HD proteins (Hobert and Westphal, 2000). Two *lim-1*-related genes have been recently identified in sea urchins (Kawasaki *et al.*, 1999) and fruit flies (Lilly *et al.*, 1999), and we suggest that they may be added to the same LIN-11 group. To the best of our knowledge, this study is the first report that describes Lim-1-like protein patterns in bivalve mollusc, sea urchin, and chick embryo tissues. Clearly, much remains to be learned about the corresponding factors involved, especially in bivalves. Nevertheless, it seems likely that the results obtained provide precedents for further identification of *lim-1*-related genes and characterization of their protein products in bivalve molluscs.

Acknowledgments

The authors thank Dr. A. A. Karavanov and Prof., Dr. I. B. Dawid for the gift of anti-XLim-1 antibodies as well as for comments and contributions at a time during which many aspects of this study were discussed and developed. We also extend our gratitude to two extremely helpful anonymous referees. The work was supported by the XUGA grant 16101A 98 from the Galicia Government to ATM and by a postdoctoral fellowship from the Institute of Health Sciences (University of La Coruña, Spain) to MT.

Literature Cited

Altschul, S. F., T. L. Madden, A. A. Schäffer, J. Zhang, Z. Zhang, W. Miller, and D. J. Lipman. 1997. Gapped BLAST and PSI-BLAST: a new generation of protein database search programs. *Nucleic Acids Res.* **25:** 3389–3402.

Bach, I. 2000. The LIM domain: regulation by association. *Mech. Dev.* **91:** 5–17.

Bairoch, A., and R. Apweiler. 2000. The SWISS-PROT protein sequence database and its supplement TrEMBL in 2000. *Nucleic Acids Res.* **28:** 45–48.

Breen, J. J., A. D. Agulnick, H. Westphal, and I. B. Dawid. 1997. Interactions between LIM domains and the LIM domain-binding protein Ldb1. *J. Biol. Chem.* **273:** 4712–4717.

Brown, S., C. Biben, L. M. Ooms, M. Maimone, M. J. McGrath, R. Gurung, R. P. Harvey, and C. A. Mitchell. 1999. The cardiac expression of striated muscle Lim protein 1 (SLIM1) is restricted to the outflow tract of the developing heart. *J. Mol. Cell Cardiol.* **31:** 837–843.

Carroll, T. J., and P. D. Vize. 1999. Synergism between *Pax-8* and *lim-1* in embryonic kidney development. *Dev. Biol.* **214:** 46–59.

Carroll, T. J., J. B. Wallingford, and P. D. Vize. 1999a. Dynamic patterns of gene expression in the developing pronephros of *Xenopus laevis*. *Dev. Genet.* **24:** 199–207.

Carroll, T. J., J. B. Wallingford, D. Seufert, and P. D. Vize. 1999b. Molecular regulation of pronephric kidney. *Curr. Top. Dev. Biol.* **44:** 67–100.

Curtiss, J., and J. S. Heiling. 1998. DeLIMiting development. *Bioessays* **20:** 58–69.

Dawid, J. B., J. J. Breen, and R. Toyama. 1998. LIM domains: multiple roles as adapter and functional modifiers in protein interactions. *Trends Genet.* **14:** 156–162.

Dong, W. F., H. H. Heng, R. Lowsky, Y. Xu, J. F. DeCoteau, and M. D. Minden. 1997. Cloning, expression, and chromosomal localization of the human LIM/HOMEOBOX gene, *hLim-1*. *DNA Cell Biol.* **16:** 671–678.

Fujii, T., J. G. Pichel, M. Taira, R. Toyama, I. B. Dawid, and H. Westphal. 1994. Expression patterns of the murine LIM class homeobox gene *lim 1* in the developing brain and excretory system. *Dev. Dyn.* **199:** 73–83.

Furuyama, T., S. Inagaki, Y. Iwahashi, and H. Takagi. 1994. Distribution of *Rlim*, an LIM homeodomain gene, in the rat brain. *Neurosci. Lett.* **170:** 266–268.

Hames, B. D. 1990. One-dimensional polyacrylamide gel electrophoresis. Pp. 1–148 in *Gel Electrophoresis of Proteins*, B. D. Hames and D. Rickwood, eds. IRL Press, Oxford.

Hancock, D. C., and G. I. Evan. 1992. Synthesis of peptides for use as immunogens. Pp. 23–32 in *Immunological Protocols*, M. Manson, ed. The Humana Press, Totowa, NJ

Hobert, O., and G. Ruvkun. 1998. A common theme for LIM homeobox gene function across phylogeny? *Biol. Bull.* **195:** 377–380.

Hobert, O., and H. Westphal. 2000. Functions of LIM-homeobox genes. *Trends Genet.* **16:** 75–83.

Hobert, O., T. d'Albert, Y. Liu, and G. Ruvkun. 1998. Control of neural development and function in a thermoregulatory network by the LIM homeobox gene *lin-11*. *J. Neurosci.* **18:** 2084–2096.

Hofmann, K., P. Bucher, L. Falquet, and A. Bairoch. 1999. The PROSITE database, its status in 1999. *Nucleic Acids Res.* **27:** 215–219.

Holland, N. D., and L. Z. Holland. 1993. Embryos and larvae of invertebrate deuterostomes. Pp. 21–32 in *Essential Developmental Biology. A Practical Approach*, C. D. Stern and P. W. H. Holland, eds. IRL Press, New York.

Karavanov, A. A., J.-P. Saint-Jeannet, I. Karavanova, M. Taira, and I. Dawid. 1996. The LIM homeodomein protein Lim-1 is widely expressed in neural, neural crest and mesoderm derivatives in vertebrate development. *Int. J. Dev. Biol.* **40:** 453–461.

Karavanov, A. A., I. Karavanova, A. Perantony, and I. Dawid. 1998. Expression pattern of the rat *lim-1* homeobox gene suggests a dual role during kidney development. *Int. J. Dev. Biol.* **42:** 61–66.

Kawasaki, T., K. Mitsunaga-Nakatsubo, K. Takeda, K. Asaka, and H. Shimada. 1999. *Lim 1* related homeobox gene (*HpLim1*) expressed in sea urchin embryos. *Dev. Growth Differ.* **41:** 273–282.

Klenova, E. M., R. H. Nicolas, A. F. Carne, R. E. Lee, V. V. Lobanenkov, and G. H. Goodwin. 1997. Molecular weight abnormalities of the CTCF transcription factor: CTCF migrate aberrantly in SDS-PAGE and the size of the expressed protein is affected by the UTRs and sequences within the coding region of the CTCF gene. *Nucleic Acids Res.* **25:** 466–474.

Li, Y. H., S. S. Cheah, J. M. Deng, W. Shawlot, and R. R. Behringer. 1999. Sequence and genomic organization of the mouse *lim1* gene. *Mamm. Genome* **10:** 444–446.

Lilly, B., D. D. O'Keefe, J. B. Tomas, and J. Botas. 1999. The LIM homeodomain protein *dlim1* defines a subclass of neurons within the embryonic ventral nerve cord of *Drosophila*. *Mech. Dev.* **88:** 195–205.

Lim, H. N., and J. R. Hawkins. 1998. Genetic control of gonadal differentiation. *Bailliere's Clin. Endocrinol. Metab.* **12:** 1–16.

Mauch, T. J., G. Yang, M. Wright, D. Smith, and G. C. Schoenwolf. 2000. Signals from trunk paraxial mesoderm induce pronephros formation in chick intermediate mesoderm. *Dev. Biol.* **220:** 62–75.

Mikhailov, A. T., and V. N. Simirsky. 1991. *Immunochemical Methods in Developmental Biology (A Manual).* Nauka, Moscow. p. 176.

Mikhailov, A. T., M. Torrado, J. Méndez, and M. J. López. 1996. Annual cycle of expression of connective tissue polypeptide markers in the mantle of the mussel *Mytilus galloprovincialis*. *Mar. Biol.* **126:** 77–89.

Mikhailov, A. T., M. Torrado, L. I. Korochkin, M. A. Kopantzeva, and J. Méndez. 1997. Male-predominant carboxylesterase expression in

the reproductive system of mollusks and insects: immunochemical and biochemical similarity between *Mytilus* male associated polypeptide (MAP) and *Drosophila* sex-specific Esterase S. *Comp. Biochem. Physiol.* **118B:** 197–208.

Newman, A. P., G. Z. Acton, E. Hartwieg, H. R. Horvitz, and P. W. Sternberg. 1999. The *lin-11* LIM domain transcription factor is necessary for morphogenesis of *C. elegans* uterine cells. *Development* **126:** 5319–5326.

Raff, R. A. 1996. *The Shape of Life: Genes, Development and the Evolution of Animal Form.* University of Chicago Press, Chicago.

Rebbert, M. L., and I. B. Dawid. 1997. Transcriptional regulation of the *Xlim-1* gene by activin is mediated by an element in intron 1. *Proc. Natl. Acad. Sci. USA* **94:** 9717–9722.

Shawlot, W., and R. R. Behringer. 1995. Requirement for *Lim1* in head-organizer function. *Nature* **374:** 425–430.

Shawlot, W., M. Wakamiya, K. M. Kwan, A. Kania, T. M. Jessell, and R. R. Behringer. 1999. *Lim 1* is required in both primitive streak-derived tissues and visceral endoderm for head formation in the mouse. *Development* **126:** 4925–4932.

Shimono, A., and R. R. Behringer. 1999. Isolation of novel cDNAs by subtractions between the anterior mesoendoderm of single mouse gastrula embryos. *Dev. Biol.* **209:** 369–380.

Sprung, M., and B. L. Bayne. 1984. Some practical aspects of fertilizing of the eggs of the mussel *Mytilus edulis* L. *J. Cons. Int. Explor. Mer* **41:** 125–128.

Taira, M., M. Jamrich, P. J. Good, and I. B. Dawid. 1992. The LIM domain-containing homeobox gene *Xlim-1* is expressed specifically in the organizer region of *Xenopus* gastrula embryos. *Genes Dev.* **6:** 356–366.

Taira, M., H. Otani, M. Jamrich, and I. B. Dawid. 1994. Expression of the LIM class homeobox gene *Xlim-1* in pronephros and CNS cell lineages of *Xenopus* embryos is affected by retinoic acid and exogastrulation. *Development* **120:** 1525–1536.

Taira, M., J.-P. Saint-Jeannet, and I. B. Dawid. 1997. Role of the *Xlim-1* and *Xbra* genes in anteroposterior patterning of neural tissue by the head and trunk organizer. *Proc. Natl. Acad. Sci. USA* **94:** 895–900.

Thompson, J. D., D. G. Higgins, and T. J. Gibson. 1994. CLUSTAL W: improving the sensitivity of progressive multiple sequence alignment through sequence weighting, position-specific gap penalties and weight matrix choice. *Nucleic Acids Res.* **22:** 4673–4680.

Torrado, M., and A. T. Mikhailov. 1998. Male-associated polypeptide (MAP) expression in different compartments of the reproductive system of the mussel *Mytilus galloprovincialis:* immunocytochemical and Western blot study. *Cell Tissue Res.* **294:** 537–547.

Toyama, R., M. L. O'Connell, C. V. E. Wright, M. R. Kuehn, and I. B. Dawid. 1995. Nodal induces ectopic *goosecoid* and *lim 1* expression and axis duplication in zebrafish. *Development* **121:** 383–391.

Tsuchida, T., M. Ensini, S. B. Morton, M. Baldassare, T. Edlung, T. M. Jessell, and S. L. Pfaff. 1994. Topographic organization of embryonic motor neurons defined by expression of LIM homeobox genes. *Cell* **79:** 957–970.

Wallingford, J. B., T. J. Carroll, and P. D. Vize. 1998. Precocious expression of the Wilms' tumor gene *xWT1* inhibits embryonic kidney development in *Xenopus laevis*. *Dev. Biol.* **202:** 103–112.